International Journal of Engineering Innovation & Research
Volume 10, Issue 6, ISSN: 2277 – 5668

Research on Tire Wear Characteristics Based on Roll and Cornering Conditions

Aiqiang Li, Congzhen Liu*, Hui Meng, Shicheng Lu, Gao Chen, Hongzhu Liu and Fei Pan
School of Transportation and Vehicle Engineering, Shandong University of Technology, 255049, Shandong, Zibo, Zhangdian, China.
*Corresponding author email id: lcz200811@163.com

Date of publication (dd/mm/yyyy): 31/12/2021

Abstract **– Tires have a variety of properties such as load-bearing performance, wear performance, grip performance, etc., and one of the important evaluation indicators is wear characteristics. This article takes 205/55R16 longitudinal groove radial tire as an example, establishes a three-dimensional tire model through Hypermesh and ABAQUS, and verifies the tire model through ground pressure test and stiffness test. Subsequently, the tire wear model under free rolling, roll, and cornering conditions was simulated. Among them, the conditions of roll and cornering are studied respectively, and the conditions of 2 degrees, 4 degrees, 6 degrees and 8 degrees are analyzed. Take the free rolling condition as the comparison condition. The results expressed that the tire wear and unevenness of grounding pressure at 6 degrees and 8 degrees under roll conditions is greater than that under free rolling conditions, and the uneven wear is aggravated on the shoulder with high pressure concentration; the tire wear and unevenness of grounding pressure in cornering conditions is much greater than that in free rolling conditions, and ground pressure is mainly distributed on the shoulders on both sides. The conclusions of the study can provide a reference for improving the wear performance of tires.**

Keywords **– Wear Characteristics, Roll, Cornering, Finite Element Analysis.**

I. INTRODUCTION

With the rapid development of automobile industry, people have higher and higher requirements for automobile driving under different composite working conditions. Therefore, the research on tire wear characteristics has attracted more and more attention from researchers at home and abroad. It is mainly divided into two aspects: the research on wear mechanism and wear calculation and evaluation methods. The research on wear mechanism has become more and more mature in recent decades; At present, the research on wear calculation and evaluation indexes mainly includes: finite element method, unit wear mileage expression method and tire wear energy calculation method. Since the wear energy loss is mainly caused by slip and does not conform to the calculation formula of classical friction mechanics, most of the methods currently used are to describe the wear from the perspective of frictional dissipation energy. The essence is to use the power per unit time to express the instantaneous wear and tear. Total wear [1]. Peng Xudong, Zhuang Jide and others elaborated on the causes of wear and described the process of tread wear. The tire wear mechanism was divided into adhesion wear, fatigue wear, and abrasive wear [2-5]. Fleischer believes that when the stored frictional energy of a certain local volume reaches a critical value sufficient to damage the surface, the local volume will be separated from the surface in the form of wear debris [6]. Cho et al. used an explicit finite element method to perform a rolling analysis of tires. Taking into account that the friction coefficient is affected by the ground pressure, they analyzed the friction loss of complex tread tires and proposed that the friction work between the tire and the ground can be used to measure the tire tread Wear [7-8]. Fan Pan used a 3D four-wheel alignment instrument and a sideslip test rig to investigate and analyze the abnormal tread wear factors. Then, he regressed the data and established a related model through simulation software to analyze the range of the positioning

angle with the wheel beating. For this kind of unreasonable runout range, a double sliding board side slip test was carried out to obtain the most ideal toe angle and a matching camber angle to reduce the amount of lateral slip and ultimately reduce abnormal wear [9].

In summary, the current domestic and foreign scholars' research on tire wear mechanism and wear calculation methods has become increasingly mature, but it is often aimed at the wear characteristics under a single working condition. Because of the influence of deflection angle and roll angle, this article will further discuss the tire wear characteristics under side slip and light side conditions.

In this paper, the basic 205 / 55R16 radial tire with longitudinal groove pattern is taken as the research object, the tire model is established based on ABAQUS, the calculation method combining finite element and wear energy dissipation method is used for reference, and the tire is modeled and analyzed under free rolling, roll and cornering conditions combined with the theoretical model, and the relevant conclusions are obtained, thus, it is convenient for researchers to better optimize the design of tire wear reduction, further effectively reduce tire wear, reduce environmental pressure and improve tire service life.

II. Tire Model Establishment and Verification

A. *Material Model*

Due to the different materials of various structures of tires, they are not entirely rubber materials. In this paper, according to the finite element deformation theory and composite material theory, the tread and sidewall structures are defined as pure rubber materials; the carcass, belt layer and other structures are defined as rubber cord composites [11]. In this paper, the Yeoh model is used to simulate the rubber material, and the constitutive equation of strain energy is shown in Eq (1) [12].

$$W = C_{10}\left(I_1 - 3\right) + C_{20}\left(I_1 - 3\right)^2 + C_{30}\left(I_1 - 3\right)^3 \tag{1}$$

Where w is the strain energy, C_{10}, C_{20}, and C_{30} are the expansion coefficients of the third-order reduction polynomial, and I_1 is the first invariant of strain.

The rubber-cord composite material is simulated by a stiffener material model composed of a basic unit and a stiffener unit Rebar, in which the attributes and direction of the cord need to be defined accordingly. The properties of the Rebar material model are shown in Table 1.

Table 1. Stiffener material properties.

Rebar Material	Young's Modulus /GPa	Poisson's Ratio	Density/Kg/m³	Angle /°
Belt steel wire 1	105.9	0.29	7800	66
Belt steel wire 2	105.9	0.29	7800	114
Carcass cord	5.25	0.3	1350	0

B. *Finite Element Model*

Taking the 205/55R16 longitudinal groove radial tire as the research object, the measured data is carried out according to the cut section of the tire, and the measured data is drawn using AutoCAD and simplified processing. Import the simplified 2D cross-section of the tire into the Hypermesh software for meshing.

Through Abaqus's *Symmetric Model Generation and other commands, the two-dimensional model is rotated once around the central axis, and the three-dimensional finite element simulation model is obtained. The modeling process is shown in Fig. 1.

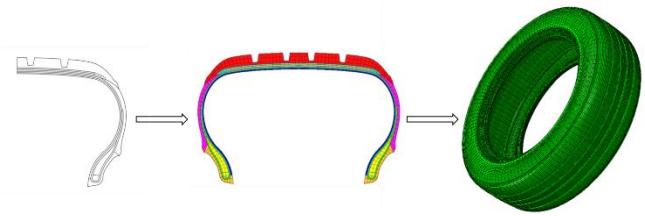

Fig. 1. Tire modeling process.

C. *Validation of Model*

After the tire meshing and material assignment are completed, use Abaqus's *Dsload command to pressurize the tire. The rated tire pressure of the sample tire is 0.26 bar. Use the *Cload command to impose an upward concentrated load on the road surface to simulate the process of tire load application. The rated load is 4000N. The validity of the model was verified from the two aspects of radial deformation and grounding footprint. The comparison of the test and simulation results of the load-sinking curve under static load is shown in Fig. 2. It can be seen from the figure that as the load increases, the sinking amount increases, but the stiffness value tends to be constant and approximate to a linear function relation.

The comparison between the tire static load test and the simulated grounding footprint shape is shown in Fig. 3. The pressure distribution of the test and the simulation diagram under the same load and air pressure has good consistency.

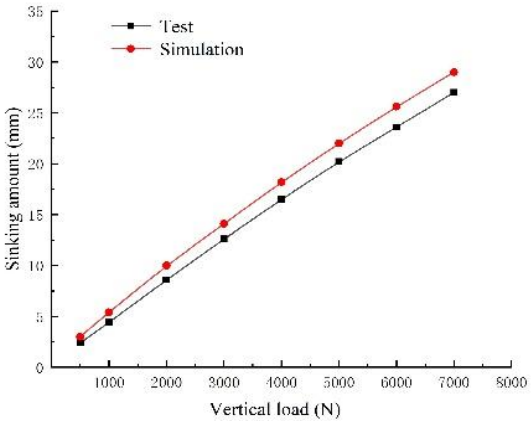

Fig. 2. load-sink curve.

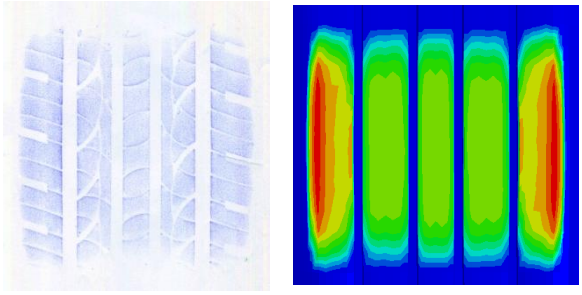

Fig. 3. Ground footprint shape under static load.

III. Evaluation Index

This article mainly uses the finite element method and the wear loss energy dissipation method to calculate the tire wear: the ground pressure value obtained by the finite element simulation is derived from the points, and then the friction is calculated using the relevant formula. At the same time, modern cars are equipped with ABS anti-lock braking systems. , This leads to a relative slip between the road surface and the tread, so the calculation of friction work cannot be calculated by braking distance. Therefore, this paper uses the frictional energy loss rate under the optimal slip ratio to characterize the tire wear performance, and uses the grounding pressure deflection value as the secondary evaluation index.

A. *Calculation of Frictional Energy Loss Rate*

Due to the existence of load, friction coefficient, and slip rate, the shear force $F_s(i,j)$ opposite to the slip speed $v(i, j)$ will be generated during braking, where i and j are the coordinates of the rubber unit, and the frictional energy loss rate when the unit slips can be expressed as Eq (2).

$$E(i,j) = F_s(i,j) \cdot v(i,j) \tag{2}$$

$$F_s(i,j) = P(i,j) \cdot A(i,j) \cdot \mu(i,j) \tag{3}$$

Where $P(i, j)$ is the ground pressure of the contact unit, $\mu(i, j)$ is the friction coefficient between the tire unit and the road surface, $A(i, j)$ is the area of the contact unit, $v(i, j)$ is the slip speed, and the slip speed is the product of the vehicle speed and the slip rate.

The area $A(i, j)$ of the contact unit can be expressed as Eq (4).

$$A(i,j) = \frac{S}{n} \tag{4}$$

Where S is the grounding area, and n is the number of effective nodes in the grounding area.

Discretely sum the frictional energy loss rate of each unit in the ground contact area, which is the total frictional energy loss rate when the tire produces slippage wear, as shown in Eq (5).

$$E = \sum_{i=1}^{n}\sum_{j=1}^{n} E(i,j) = \mu(i,j)\sum_{i=1}^{n}\sum_{j=1}^{n} p(i,j) \cdot v(i,j) \cdot A(i,j) \tag{5}$$

B. *Calculation of Grounding Pressure Deflection Value*

The ground pressure deflection value mainly refers to the evaluation of whether the tread ground pressure distribution is uniform, which belongs to an important wear evaluation index, as shown in Eq (6).

$$\alpha = \sqrt{\frac{1}{n-1}\sum_{i=1}^{n}(P_i - \bar{P})^2} \tag{6}$$

Where, P_i is the pressure value of a point (i, j) in the grounding area, n is the number of effective nodes in the area, and $\bar{P}$ is the mean value of pressure distribution in the grounding area.

IV. Simulation Analysis Of Wear Under Roll and Cornering Conditions

In actual driving, car tires will be under different loads, tire pressures, slip angles, and roll angles. When the

tires are affected by these variables, they will be in different working conditions, resulting in uneven wear. This section uses free rolling as the basic working conditions to study the wear of tires under different slip angles and roll angles. The rated load is 4000N and the standard tire pressure is 0.26Mpa.

A. *Free Rolling Condition*

Free rolling is the most common and most basic working condition of tires. Accurately studying this working condition is the prerequisite for the correct simulation analysis of other working conditions below.

The driving speed set in this article is 60Km/h. First, calculate the free rolling angular velocity range of the tire by estimating the rolling radius of the tire, and then obtain the relationship curve between the longitudinal friction force and the rolling angular velocity by controlling the rolling angular velocity of the tire, as shown in Fig. 4. When the force is zero, the tire is in a free rolling state, and its free rolling angular velocity is 53.7905rad/s.

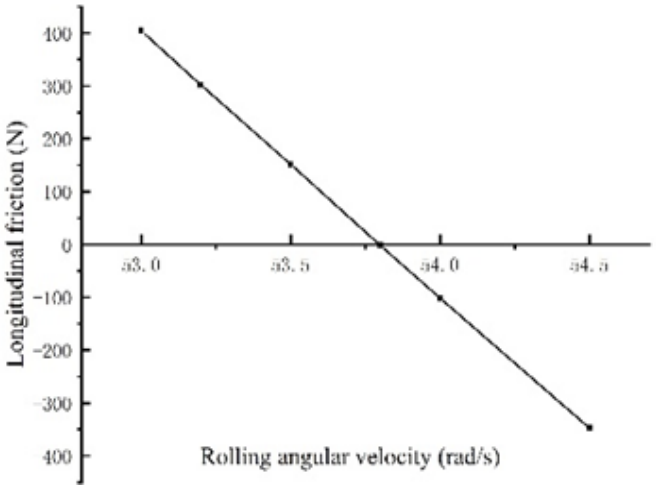

Fig. 4. The relationship between longitudinal friction and rotational angular velocity.

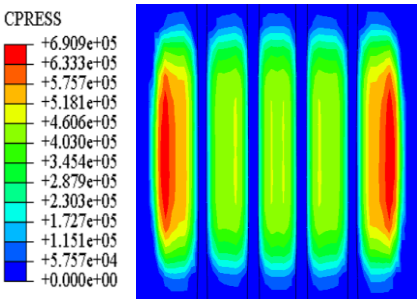

Fig. 5. Ground footprint shape in free rolling condition.

The grounding footprint diagram of the tire in the free rolling state is shown in Fig. 5. The overall shape of the grounding footprint is rectangular, and the grounding pressure is concentrated on the shoulders on both sides. The simulation analysis results in the free rolling state are shown in Table 2.

Table 2. Simulation analysis results under free rolling conditions.

Free rolling Conditions	**Friction Energy Loss Rate (J/s)**	**Grounding Pressure Deflection Value (Mpa)**	**Grounding Area (cm^2)**
	10627.8835	0.1297	147.06

B. *Roll Conditions*

The car body generally uses three important attributes to characterize its movement on the ground, that is, the rotation through the X/Y/Z three directions of the center of mass, which respectively refer to the roll around the X axis, the pitch around the Y axis, and the rotation around the Y axis. The yaw movement of the Z axis. Regardless of extreme circumstances, roll around the X axis is a relatively common working condition, mainly due to the centrifugal force when the car turns, and the wheel and the road remain relatively stationary in the normal direction of the turn, and the center of gravity of the body still tends to be centrifugal., Which leads to the tendency of the car body to turn outwards around the X direction and roll. This article studies the roll conditions, and sets the conditions of 2 degrees, 4 degrees, 6 degrees, and 8 degrees for specific analysis.

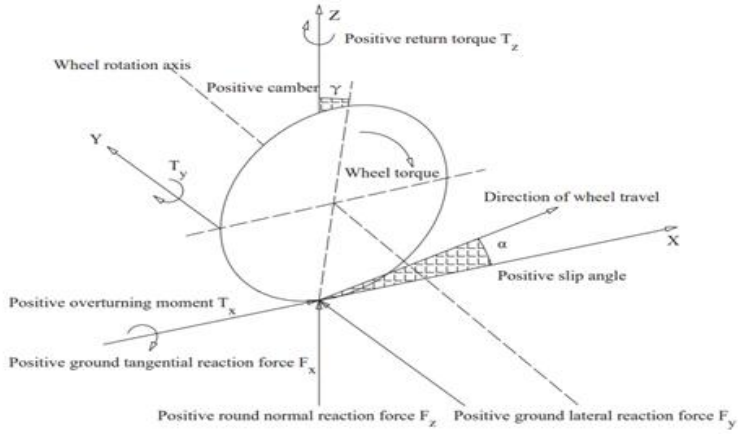

Fig. 6. Tire coordinate system diagram.

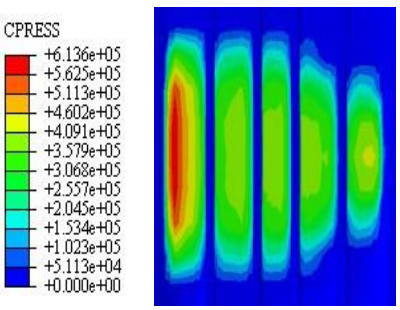

Fig. 7. Ground footprint shape of roll 2 degrees.

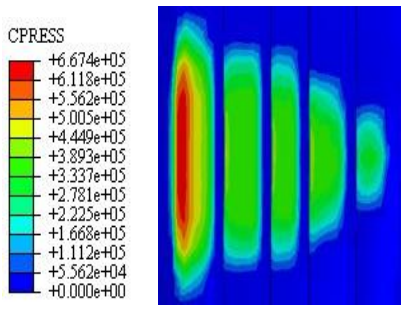

Fig. 8. Ground footprint shape of roll 4 degrees.

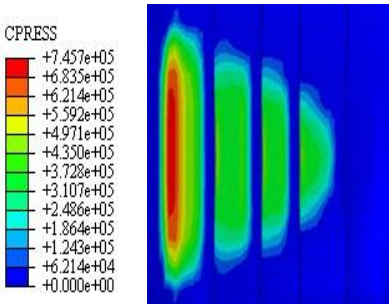

Fig. 9. Ground footprint shape of roll 6 degrees.

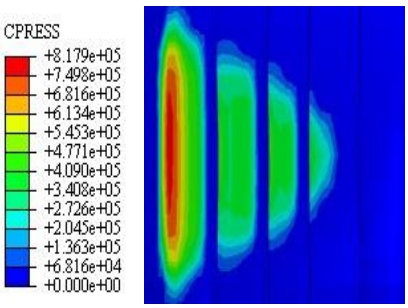

Fig. 10. Ground footprint shape of roll 8 degrees.

The ground pressure diagram after Abaqus simulation analysis is shown in the figure above.

From the ground pressure diagram, when the roll angle does not exceed 4 degrees, the ground pressure is less than the free rolling condition, and the ground pressure is distributed asymmetrically, only on one side of the

shoulder, which is more in line with the actual situation. With the increase of the roll angle, the ground pressure increases faster, and the pressure difference between the shoulders on both sides gradually increases. The ground contact marks show a slender trend, and the overall shape becomes a triangle, indicating that the ground pressure is highly concentrated on one side of the tire. Shoulder, aggravate the uneven wear of the tire.

Table 3. Simulation analysis results under roll conditions.

Angle (°)	Friction Energy Loss Rate (J/s)	Grounding Pressure Deflection Value (Mpa)	Grounding Area (cm2)
2	10625.6639	0.1486	148.48
4	10676.4361	0.1625	142.13
6	10693.6546	0.1788	131.67
8	10794.7742	0.1874	127.59

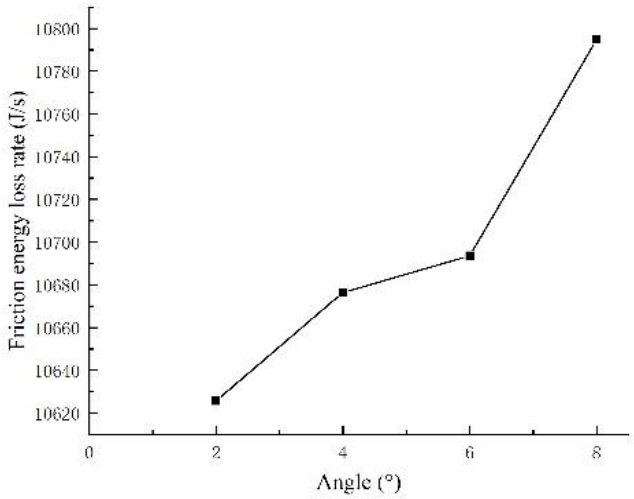

Fig. 11. Frictional energy loss rate under different angles.

The frictional energy loss rate and ground pressure skewness values calculated by extracting relevant data are shown in Table 3. It can be seen from the chart data of the evaluation index that the tire wear in the roll condition is greater than that in the free rolling condition, and the uniformity of the ground pressure distribution is worse. When the roll angle is 2 degrees, the tire contact area is the largest and most uniform. As the angle increases, the contact area becomes smaller and the footprint becomes extremely uneven. Fig. 11 shows that as the roll angle increases, the tire wear energy loss rate increases, and the wear performance becomes worse.

C. *Cornering Condition*

The lateral force Fy on the ground against the tire caused by the steering, road slope, lateral wind, etc. along the Y axis at the center of the wheel is called the cornering force, and its direction is always directed to the inside of the turn. And because the elastic tire has a certain degree of lateral elasticity, the side deviation force (even if it fails to reach its adhesion limit) will cause the wheel to deviate from the wheel plane and cause side deviation, as shown in Fig. 6. Due to the presence of this cornering force, the tire will have a cornering angle similar to that shown in Fig. 12. It is defined as the angle between the longitudinal speed and the direction of the resultant speed, as shown in formula (7).

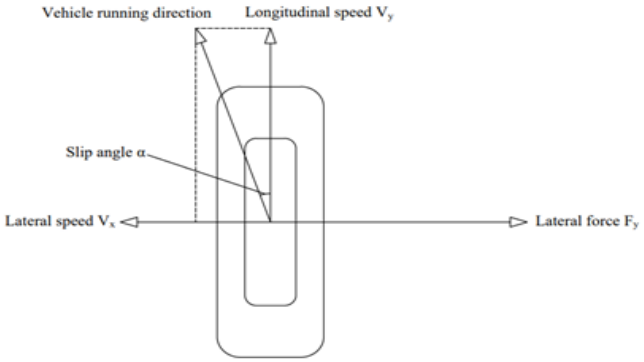

Fig. 12. Schematic diagram of slip angle.

The ground pressure diagram under different slip angles is shown in the figure below.

From the ground pressure diagram, it can be seen that the ground pressure distribution under the side slip condition and the free rolling condition is similar, but the difference is that the ground pressure at the shoulder part of the side slip condition is greater and the maximum ground pressure area is transferred to the edge of the ground center rib pattern. Specifically, as the cornering force increases, the ground contact pressure gradually increases, and the overall shape of the ground contact mark changes from a rectangle to a trapezoid, showing a trend of increased wear on one side of the shoulder and slower wear on the other side. This is consistent with the actual situation of tire driving under cornering conditions.

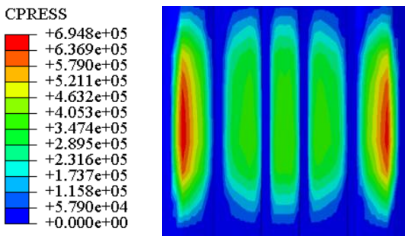

Fig. 13. Ground footprint shape of cornering 2 degrees.

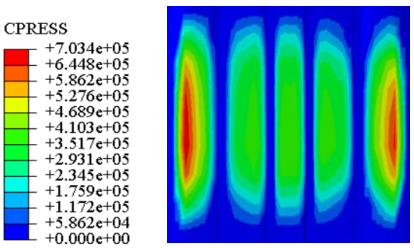

Fig. 14. Ground footprint shape of cornering 4 degrees.

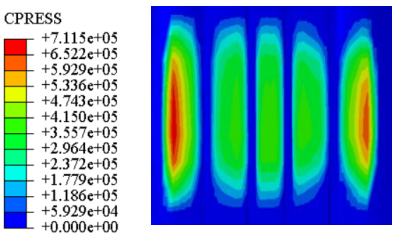

Fig. 15. Ground footprint shape of cornering 6 degrees.

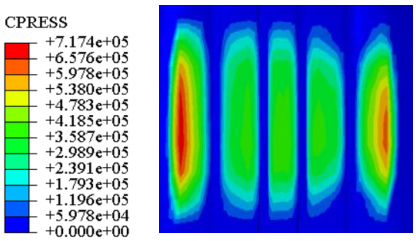

Fig. 16. Ground footprint shape of cornering 8 degrees.

Table 4. Simulation analysis results under cornering conditions

Angle (°)	Lateral Force (N)	Friction Energy Loss Rate (J/s)	Grounding Pressure Deflection Value (Mpa)	Grounding Area (cm^2)
2	653	10641.7852	0.1326	146.48
4	1256	10678.4531	0.1401	137.23
6	1879	10707.4557	0.1649	139.88
8	2142	10727.1538	0.1713	136.97

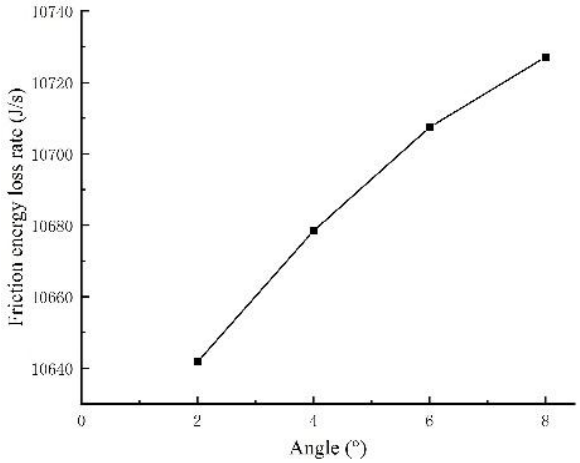

Fig. 17. Frictional energy loss rate under different angles

Extract the relevant data to calculate the frictional energy loss rate and ground pressure skewness as shown in Table 4. From the chart data of the evaluation index, it can be seen that the tire wear in the cornering condition is greater than that in the free rolling condition, and the uniformity of the ground pressure distribution is also worse. It can be seen from Fig. 17 that as the cornering angle increases, the frictional energy loss rate of the tire increases.

V. CONCLUSION

This paper uses the finite element software ABAQUS for modeling, and verifies the validity of the model through grounding experiments. Then carry out the simulation analysis of free rolling conditions, roll conditions, and side slip conditions. The free rolling conditions are control conditions, and the angles of roll and roll are set to 2 degrees, 4 degrees, 6 degrees, and 8 degrees. The results show that the ground pressure is not symmetrically distributed and highly concentrated on one side of the shoulder, and the overall shape of the ground contact mark changes from a trapezoid to a triangle; in a sideways working condition, the maximum grounding pressure increases with the increase of the side yaw force. The pressure area shifts to the edge of the rib pattern in the grounding center, and the overall shape of the grounding footprint changes from a rectangle to a triangle, showing a trend of increased wear on one side of the shoulder and slower wear on the other side. The results of the study can provide a reference for the study of tire wear performance.

REFERENCES

[1] Xiu-lei Fan, Zi-xuan Ma, Ye-feng Zou, Jia-qiang Liu, Jun Hou. Investigation on the adsorption and desorption behaviors of heavy metals by tire wear particles with or without UV ageing processes [J], Environmental research, 2021, 195.
[2] Xu-dong Peng, Kong-hui Guo, Yu-hua Ding, Influencing factors of tire wear [J], Rubber industry, 2003, 10 (50): 619-624.
[3] Xu-dong Peng, You-bai Xie, Kong-hui Guo, Research and development of tire Tribology [J], China Mechanical Engineering, 1999 (2): 215-219.
[4] Xu-dong Peng, You-bai Xie, Kong-hui Guo, Study on wear mechanism of automobile tire [J], Lubrication and sealing, 1999 (6): 50-52.
[5] Ji-de Zhuang, Modern automobile tire technology [M], Beijing: Beijing University of Technology Press, 2001.
[6] Yun-min Zhu, Rubber wear principle [J], Lubrication and sealing, 1998 (05):.14.
[7] Cho J. C., Jung B. C.. Prediction of tread pattern wear by an explicit finite element model [J], Tire Science and Technology, 2007, 35 (4): 276-299.
[8] Cho J.R., Choi J.H. and Kim Y.S. Abrasive wear amount estimate for 3D patterned tire utilizing frictional dynamic rolling analysis [J], Tribology International, 2011, 44 (7): 850-858.
[9] Pan Fan,The Research on the Influence of Wheel Alignment Parameters on Tire Wear [M], Qingdao University of Technology, 2015.
[10] Rui-jin Qian, Hao Cheng, Finite element analysis on cornering characteristics of truck and bus radial Tire, Tire industry, 2021,41 (03): 143-147.
[11] Zhen Yao, Modeling and contact features investigation of radial tire utilizing ABAQUS [D], Ningbo University, 2015.
[12] Jun Wang, Liang Li, Lin Sun. Finite element analysis of 245/70R16 tires [J]. Tire Industry.2016, (9): 520-528.

AUTHOR'S PROFILE

First Author
Aiqiang Li, Master in reading, Male, School of Transportation and Vehicle Engineering, Shandong University of Technology, Shandong, Zibo, Zhangdian, 255049, China. email id: laq199897@163.com

Second Author
Congzhen Liu, Doctor of Engineering, Male, Associate Professor, School of Transportation and Vehicle Engineering, Shandong University of Technology, (Correspondence author), Shandong, Zibo, Zhangdian, 255049, China.

Third Author
Hui Meng, Master in reading, Male, School of Transportation and Vehicle Engineering, Shandong University of Technology, 255049, Shandong, Zibo, Zhangdian, China.

Fourth Author
Shicheng Lu, Master in reading, Male, School of Transportation and Vehicle Engineering, Shandong University of Technology, Shandong, Zibo, Zhangdian, 255049, China.

Fifth Author
Gao Chen, Master in reading, Male, School of Transportation and Vehicle Engineering, Shandong University of Technology, Shandong, Zibo, Zhangdian, 255049, China.

Sixth Author
Hongzhu Liu, Master in reading, Male, School of Transportation and Vehicle Engineering, Shandong University of Technology, Shandong, Zibo, Zhangdian, 255049, China.

Seventh Author
Fei Pan, Master, Female, Department of Vehicle Operation Engineering, Yantai Automobile Engineering Professional College, Shandong, Yantai, Fushan, 265500, China.